*Iraqi Journal of Physics, 2026*
*https://doi.org/10.30723/ijp.v24i2.1436*

*Vol.24, No.2, PP.80-86*
*P-ISSN: 2070-4003*
*E-ISSN: 2664-5548*

# Studying the Effect of Oxygen on the Geometrical, Electronical and Thermodynamics Properties of $SnO_2$ Pyramid using Density Functional Theory

**Hawraa M. Esaed[1*] and Mohammed T. Hussein[1]**
[1]*Department of Physics, College of Science, University of Baghdad, Baghdad, Iraq*
[*]Corresponding author: hawraa.mahmoud2304@sc.uobaghdad.edu.iq

## Abstract
Light atoms, such as oxygen, are treated with the 6-311G** basis sets, and heavy atoms, like tin (Sn), are treated with SDD (Stuttgart/Dresden) basis sets. A density functional theory (DFT) with a B3LYP hybrid functional calculation needs to be done to work out the geometrical and electronic properties, such as the highest occupied molecular orbital (HOMO), the lowest unoccupied molecular orbital (LUMO), and the energy gap, as well as the thermodynamic properties, such as Gibbs free energy, enthalpy, entropy, and heat capacity of the tin dioxide ($SnO_2$) pyramid nanocluster structure as a function of the number of oxygen atoms. These theoretical calculations were performed using Gaussian 09W, while the geometry was visualized using Gaussian View 05. It was found that the $SnO_2$ pyramid nanocluster energy gap in the beginning increased with the increase of the oxygen atoms and reached a maximum at $Sn_{10}O_{16}$, then dropped to a minimum value at 2.55 eV for $Sn_{10}O_{17}$. The Gibbs free energy and enthalpy values became more negative, indicating that the reaction was exergonic.

**Article Info.**

**Keywords:**
*Tin Dioxide, Electronic Properties, Density of State, Gaussian 09W, Density Functional Theory (DFT).*

**Article history:**
*Received: Feb. 09, 2025*
*Revised: May, 06, 2025*
*Accepted:May, 13, 2026*
*Published:Jun. 01,2026*

## 1. Introduction
The n-type semiconductor tin dioxide ($SnO_2$) has a bandgap of 3.4-3.6 eV. It is not only highly transparent and chemically stable but also mechanically stable, which makes it preferable for dye-sensitized solar cells, various gas sensors, the industry of optoelectronics, electrochromic devices, and electrodes. Although $SnO_2$ has been a favourite option among gas sensors due to its high charge carriers' mobility and their reliable chemical and thermal resistance, this material has hardly been used as a chemical sensor for heavy metal ions in an aqueous condition [1-7]. A broad spectrum of oxides has characteristics of electrical properties that change under the effect of oxidizing and reducing gases, and have gained widespread sensitivity against oxidizing and reducing gases. Of those, $SnO_2$ has been, for many years, the most promising and also the most widely used in practical applications. $SnO_2$ stands out by having two main properties: high gas-type sensitivity and low cost. Many doping materials can be utilized for $SnO_2$ gas sensors to get faster response time, lower operation temperature, and be more selective [8-14].

In a previous study, Jafer and Hussein investigated $SnO_2$ as a nitrogen gas sensor. Using density functional theory (DFT), which is a method that uses an electron density to calculate the physical properties and compare with experimental results, the $B_3LYP$ level, with 6-311G** basis sets for light atoms like nitrogen and oxygen, and SDD basis sets for heavy atoms like tin. The transition state of the $SnO_2$ nanocluster with $NO_2$ gas molecules was determined. These simulations were conducted via Gaussian 09W across a temperature range of 273 to 373 K, yielding the activation and reaction values for Gibbs free energy, enthalpy, and entropy [15].

Additionally, DFT has been utilized to p-n heterojunction of $SnO_2$ nanoparticles/reduced graphene oxide as a sensor for $NO_2$ gas. This work demonstrated that gas interaction with the $SnO_2$ surface is energetically more favourable than rGO edges due to lower Gibbs free energy, aligning well with existing literature [16,17]. While our previous work focused on establishing a theoretical foundation for these materials in various applications, such as a sensor or photo detector. In the present work, $SiO_2$ with a varying oxygen atom content was used as a humidity sensor.

## 2. Methodology

The structure and various properties of the sensing materials were analysed using the $B_3LYP$ (Becke three-parameter, Lee-Yang-Parr) level of DFT. The 6-311G** basis set was applied for lighter atoms like oxygen, while the Stuttgart/Dresden (SDD) basis set was used for heavier atoms like tin. The Gaussian 09W molecular software was employed during the calculations, along with the Gaussian View 05, which was used as a supplementary tool to look at the geometric structure [18 -25], as presented in Fig. 1.

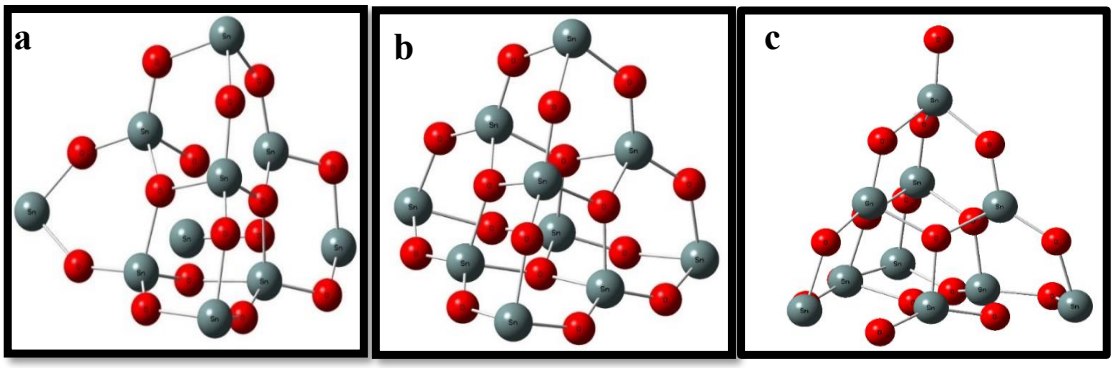


***Figure 1: Geometrical optimization of (a) $Sn_{10}O_{15}$, (b) $Sn_{10}O_{16}$ and (c) $Sn_{10}O_{17}$.***

## 3. Results and Discussion

### 3.1. Electronics Properties

The energy gap difference between the levels of the Highest Occupied Molecular Orbital (HOMO) and the Lowest Unoccupied Molecular Orbital (LUMO) was determined through Eq. (1):

$$E_g = |\mathrm{LUMO} - \mathrm{HOMO}| \qquad (1)$$

Fig. 2 demonstrates the energy levels of the HOMO and the LUMO for (a) $Sn_{10}O_{15}$, (b) $Sn_{10}O_{16}$, and (c) $Sn_{10}O_{17}$ with the variation of the number of oxygen atoms (O).

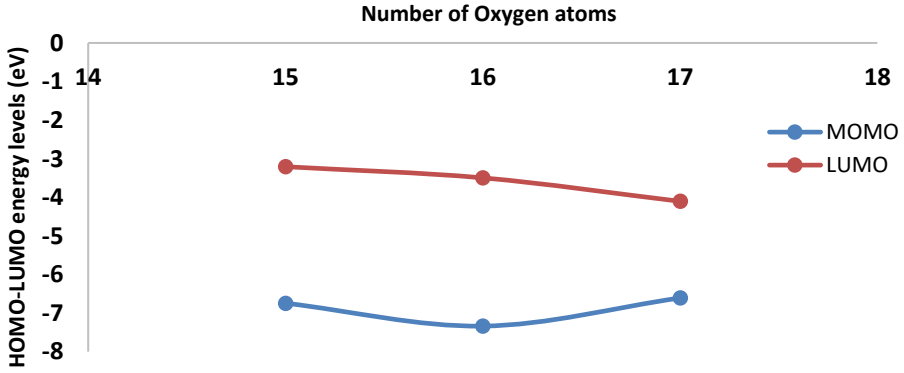


***Figure 2: Energy levels HOMO and LUMO of Tin dioxide as a function of different number. of oxygen atoms.***

Fig. 3 shows the density of state of (a) $Sn_{10}O_{15}$, (b) $Sn_{10}O_{16}$, and (c) $Sn_{10}O_{17}$ as a function of the energy levels. The energy gap between the HOMO was calculated from Eq. (1) to be 3.566, 3.841, and 2.505 eV, respectively.

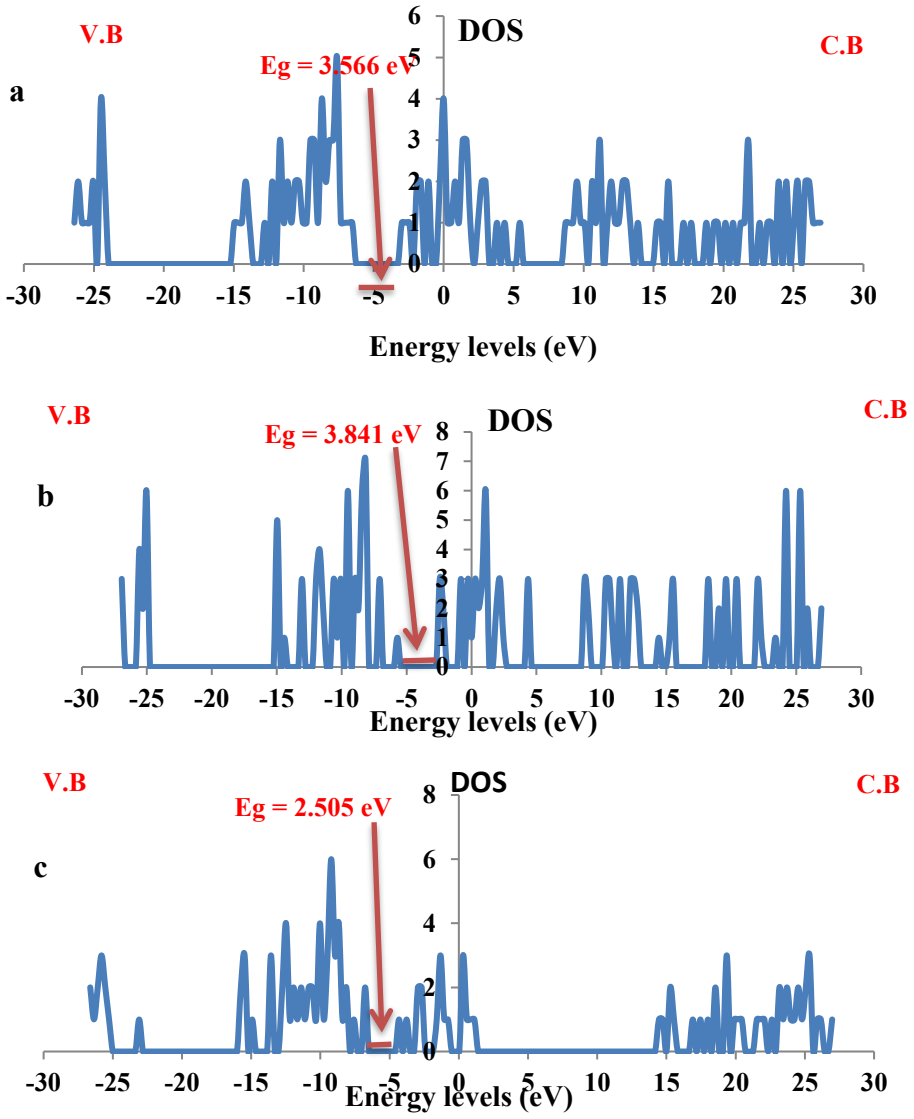


***Figure 3: Density of states for (a) $Sn_{10}O_{15}$, (b) $Sn_{10}O_{16}$ (c) $Sn_{10}O_{17}$.***

Fig. 4 shows the relation between the calculated energy gap, taken as 3.6, 3.8 and 2.5 eV for tin dioxide and the number of oxygen atoms.

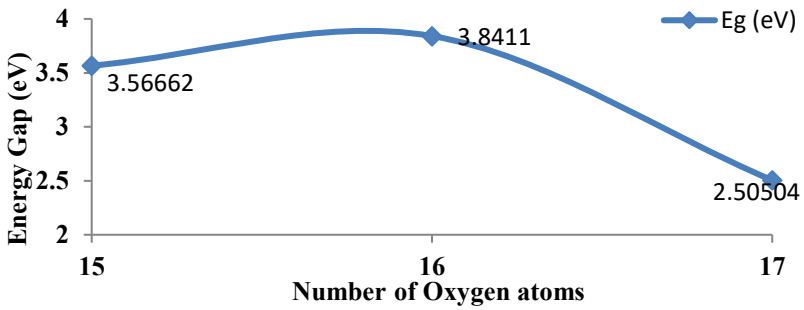


***Figure 4: Energy gap for (a) $Sn_{10}O_{15}$, (b) $Sn_{10}O_{16}$ (c) $Sn_{10}O_{17}$ as a function of the number of oxygen atoms.***

### 3.2. Thermodynamic Properties

Fig. 5a and b show Gibbs free energy and Enthalpy as a function of the number of oxygen atoms. It was found that the values increased (in negative sign), which indicates that the reaction is exergonic, according to Eq. (2) [26-28].

$$\Delta G = \Delta H - \Delta ST \quad (2)$$

Fig. 5 (c, d) shows the entropy and specific heat capacity as a function of the number of oxygen atoms. It was found that the values increased according to Eqs. (2 and 3):

$$C = \frac{Q}{m.\Delta T} \quad (3)$$

where C is the specific heat capacity, Q is the amount of heat, m is the mass of the sample, and ΔT is the temperature difference.

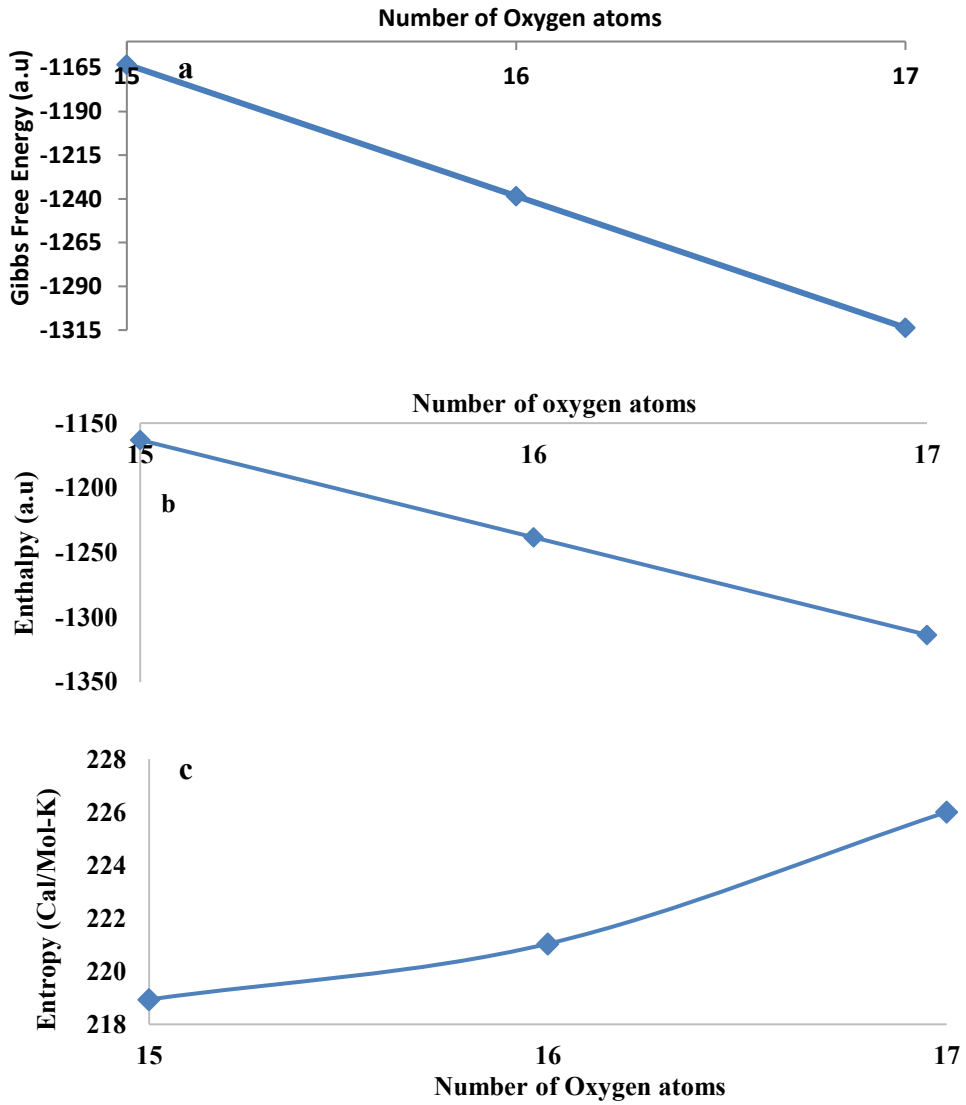

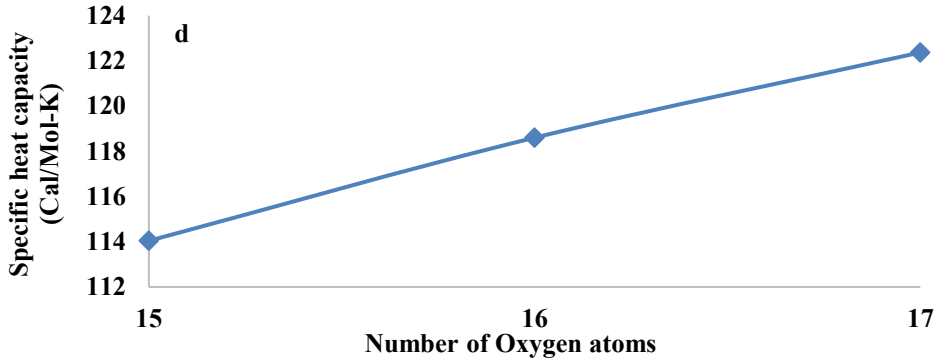


***Figure 5: Thermodynamic properties for (a) $Sn_{10}O_{15}$, (b) $Sn_{10}O_{16}$ (c) $Sn_{10}O_{17}$ as a function of the number of oxygen atoms.***

## 4. Conclusions

DFT with $B_3LYP$ hybrid functional was used to calculate the electronic and thermodynamic properties of tin oxide as a function of the number of oxygen atoms. The tin oxide pyramid nanocluster interacting with oxygen was explained in terms of geometry. The magnitude of the energy gap was concluded from the molecular orbital HOMO and LUMO to obtain the response value of oxygen as a gas sensor. The Gibbs free energy and enthalpies were negative, meaning the reactions were exergonic. The fact that both the entropy and heat capacity values were positive indicates that the structure was unstable thermodynamically.

## Conflict of interest

The authors declare that they have no conflict of interest.

## References

1. M. Hettenbach, PhD thesis, University of Tubinge, Germany (2000).
2. Y. Xu, L. Zheng, C. Yang, X. Liu, and J. Zhang, Highly Sensitive and Selective Electronic Sensor Based on CO Catalyzed $SnO_2$ Nanospheres for Acetone Detection, *Sens. Actuators B: Chem.* **304**, 127237 (2020). https://doi.org/10.1016/j.snb.2019.127237.
3. H. Zhang, J. Qian, J. Zhang, and J. Xu, Enhancing the Electrochemical Activity and Stability of Sb $SnO_2$ Based Electrodes by the Introduction of Nickel Oxide, *J. Alloys Comp.* **882**, 160700 (2021). https://doi.org/10.1016/j.jallcom.2021.160700.
4. L. Song, B. Zhao, X. Ju, L. Liu, Y. Gong, W. Chen, and B. Lu, Comparative Study of Methanol Gas Sensing Performance for $SnO_2$ Nanostructures by Changing their Morphology, *Mater. Sci. Semicond. Process.* **111**, 104986 (2020). https://doi.org/10.1016/j.mssp.2020.104986.
5. M. Kaur, D. Prasher, and R. Sharma, Recent Developments on I and II Series Transition Elements Doped $SnO_2$ Nanoparticles and its Applications For Water Remediation Process: A Review, *J. Water Environ. Nanotechnol.* **7**(2), 194 (2022). https://doi.org/10.22090/jwent.2022.02.007.
6. Y. Huang, S. Li, Chaorong Wu, S. Wang, C. Wang, and R. Ma, Introduction of LiCl Into $SnO_2$ Electron Transport Layer for Efficient Planar Perovskite Solar Cells, *Chem. Phys. Lett.* **745**, 137220 (2020). https://doi.org/10.1016/j.cplett.2020.137220.
7. X. Xu, X. Liu, H. Du, W. Zhang, S. Wang, and C. Sun, Hydrogen Bonding State of THF-$H_2O$ Solution Analyzed by 2D Raman-COS Spectroscopy, *Opti. Express.* **32**(27), 48174 (2024). https://doi.org/10.1364/OE.539683.
8. X. Lan, J. Cui, X. Zhang, R. Hu, L. Tan, J. He, H. Zhang, X. Yu Xiong, X. Yang, S. Wu, and M. Zhu, Boosting Reversibility and Stability of Li Storage in $SnO_2$–Mo Multilayers: Introduction of Interfacial Oxygen Redistribution, *Adva. Mater.* **34**(9), 2106366 (2022). https://doi.org/10.1002/adma.202106366.
9. A. L. Errico, Ab initio FP-LAPW study of the semiconductors SnO and $SnO_2$, *Phys. B: Condens. Matter.* **389** (1), 140 (2007). https://doi.org/10.1016/j.physb.2006.07.041.
10. L. Gracia, A. Beltran, and J. Andres, Characterization of the High-Pressure Structures and Phase Transformations in $SnO_2$. A Density Functional Theory Study, *J. Phys. Chem. B*, **111**(23), 6479 (2007). https://doi.org/10.1021/jp067443v.
11. X. Liu, N. Chen, B. Han, X. Xiao, G. Chen, I. Djerdj, and Y. Wang, Nanoparticle Cluster Gas Sensor: Pt Activated $SnO_2$ Nanoparticles for $NH_3$ Detection with Ultrahigh Sensitivity, *Nanoscale.* **7**(36), 14872 (2015). https://doi.org/10.1039/C5NR03585F.

12. D. Chen, J. Xu, Z. Xie, and G. Shen, Nanowires Assembled $SnO_2$ Nanopolyhedrons with Enhanced Gas Sensing Properties, *ACS Appl. Mater. Interfaces*. **3**(6), 2112 (2011). https://doi.org/10.1021/am2003312.
13. B. Wang, L. F. Zhu, Y. H. Yang, N. S. Xu, and G. W. Yang, Fabrication of a $SnO_2$ Nanowire Gas Sensor and Sensor Performance for Hydrogen, *J. Phys. Chem. C*, **112**(17), 6643 (2008). https://doi.org/10.1021/jp8003147.
14. L. Wang, Z. Lou, T. Zhang, H. Fan, and X. Xu, Facile synthesis of hierarchical $SnO_2$ semiconductor microspheres for gas sensor application, Sen. Actuators B: Chem. **155**(1), 285 (2011). https://doi.org/10.1016/j.snb.2010.12.036.
15. N. F. Jafer and M. T. Hussein, Study of the Transition State of $SnO_2$ Cluster with $NO_2$ Gas Molecule via Density Functional Theory, *Int. J. Nanosci.* **21**(01), 2250006 (2022). https://doi.org/10.1142/S0219581X22500065.
16. S. Tingting, Z. Fuchun, and Z. Weihu, Density functional theory study on the electronic structure and optical properties of $SnO_2$, *Rare Metal Mat. Eng.* **44**(10), 2409 (2015).https://doi.org/10.1016/S1875-5372(16)30031-5.
17. J. Kujawski, K. Czaja, E. Jodlowska, K. Dettlaff, M. Politanska, J. Zwawiak, R. Kujawski, T. Ratajczak, and M. K. Chmielewski, M. K. Bernard, Structural and Spectroscopic Properties of Econazole and Sulconazole – Experimental and Theoretical Studies, *J. Mol. Struct.* **1119**, 250 (2016). https://doi.org/10.1016/j.molstruc.2016.04.065.
18. J. Kujawski, K. Czaja, E. Jodlowska, K. Dettlaff, M. Politanska, J. Zwawiak, R. Kujawski, T. Ratajczak, and M. K. Chmielewski, M. K. Bernard, Structural and Spectroscopic Properties of Econazole and Sulconazole – Experimental and Theoretical Studies, *J. Mol. Struct.* **1119**, 250 (2016). https://doi.org/10.1016/j.molstruc.2016.04.065.
19. M. A. Abdulsattar, H. H. Abed, R. H. Jabbar, and N. M. Almaroof, Effect of Formaldehyde Properties on $SnO_2$ Clusters Gas Sensitivity: A DFT Study, *J. Mol. Graph. Model.* **102**, 107791 (2021). https://doi.org/10.1016/j.jmgm.2020.107791.
20. A. H. Raheem, K. J. Al-Shejyri, and E. D. Al-Bermany. Density Functional Theory Calculations for Methyl Benzene Molecule Group, *Br.J. Sci.* **5**(2), 57 (2012).
21. P. Verma and D. G. Truhlar, Status and Challenges of Density Functional Theory, Trends Chem. **2**(4), 302 (2020). https://doi.org/10.1016/j.trechm.2020.02.005.
22. P. Geerlings, E. Chamorro, P. K. Chattaraj, F. De Proft, J. L. Gázquez, S. Liu, C. Morell, A. Toro-Labbé, A. Vela, and P. Ayers, Conceptual Density Functional Theory: Status, Prospects, Issues, *Theor. Chem. Acc.* **139**(2), (2020). https://doi.org/10.1007/s00214-020-2546-7.
23. A. Ur Rahman, D. M. Saaduzzaman, S. M. Hasan, and M. K. U. Sikder, A comparative DFT study of structural, electronic, thermodynamic, optical, and magnetic properties of TM (Ir, Pt, and Au) doped in small Tin ($Sn_5$ & $Sn_6$) clusters, *Phase Transit.* **95**(7), 486 (2022). https://doi.org/10.1080/01411594.2022.2080065.
24. S. Boy, G. Kotan, and H. Yuksek. Calculation of Some Theoretical Properties of 3-(p-Methoxybenzyl)-4-(4-Hydroxybenzylidenamino)-4,5-Dihydro-1H-1,2,4-Triazol-5-One with DFT, in *The Eurasia Proceedings of Science Technology Engineering and Mathematics*, **20,** 120 (2022). https://doi.org/10.55549/epstem.1222679.
25. T. T. Khalaf and M. T. Hussein, Thermodynamic and Spectroscopic Properties Investigation of Coronene as a Function of the Number of Oxygen Atoms and Temperature via Density Functional Theory, *Iraqi J. Phys.* **22**(2), 81 (2024). https://doi.org/10.30723/ijp.v22i2.1239.
26. M. A. Abdulsattar, R. H. Jabbar, and M. A. Al-Seady, Ethanol properties effects on its reaction with Mo-doped $SnO_2$ clusters: A gas sensor model, *Results Surf. Interfaces.* **17**, 100291 (2024). https://doi.org/10.1016/j.rsurfi.2024.100291.
27. M. A. Abdulsattar, Pristine and Ni-doped $In_2O_3$ pyramids response to $NO_2$ gas: a transition state theory study, *Interactions.* **246,** 62 (2025). https://doi.org/10.1007/s10751-025-02282-z.
28. M. A. Abdulsattar, $NO_2$ properties that affect its reaction with pristine and Pt-doped $SnS_2$: a gas sensor study, *J. Mol. Model.* **30**, 417 (2024). https://doi.org/10.1007/s00894-024-06223-5.

# دراسة تأثير الاوكسجين على الخواص التركيبية والالكترونية والحرارية لاوكسيد القصدير الهرمي بأستخدام نظرية دالية الكثافة

**حوراء محمود اسعيد[1] ومحمد تقي حسين[1]**
*[1] قسم الفيزياء، كلية العلوم، جامعة بغداد، بغداد، العراق*

## الخلاصة
تمت معالجة الذرات الخفيفة مثل الاوكسجين بمجموعات الأساس 6-311G** وتم التعامل مع الذرات الثقيلة مثل القصدير (Sn) بمجموعات أساس SDD (شتوتغارت/دريسدن) من خلال استخدام نظرية دالية الكثافة (DFT) مع الدالة الهجينة B3LYP لتحديد الخصائص الهندسية والإلكترونية، مثل أعلى مدار جزيئي مشغول (HOMO)، وأدنى مدار جزيئي غير مشغول (LUMO)، وفجوة الطاقة بالإضافة إلى الخصائص الديناميكية الحرارية مثل طاقة جيبس الحرة والانثالبي والإنتروبي والسعة الحرارية للتركيب النانوي الهرمي لثاني أكسيد القصدير $SnO_2$ كدالة لعدد ذرات الاوكسجين. تم إجراء هذه الحسابات النظرية باستخدام Gaussian 09W في حين تم الحصول على الشكل الهندسي الفراغي بواسطة Gaussian View 05. وقد وجد أن فجوة الطاقة $SnO_2$ زادت في البداية مع إضافة ذرات الاوكسجين ووصلت إلى الحد الأقصى عند $Sn_{10}O_{16}$ ثم انخفضت إلى القيمة الادنى 2.50 الكترون فولت عند $Sn_{10}O_{17}$. بينما أصبحت طاقة جيبس الحرة وقيم الانثالبي أكثر سلبية، وهذا يعني أن التفاعل لا يزال باعثا للطاقة.

**الكلمات المفتاحية:** ثنائي اوكسيد القصدير، الخواص الالكترونية، كثافة الحالات، برنامج Gaussian 09W، نظرية دالية الكثافة.